THE ASTROPHYSICAL JOURNAL, 470:L53–L56, 1996 October 10

THE NEW AM HERCULIS–TYPE OBJECT AX J2315−592 DISCOVERED WITH *ASCA*

KAZUTAMI MISAKI,[1] YUICHI TERASHIMA,[1] YUICHI KAMATA,[1] MANABU ISHIDA,[2] HIDEYO KUNIEDA,[1] AND YUZURU TAWARA[1]
Received 1996 April 22; accepted 1996 July 15

ABSTRACT

The new AM Her–type object AX J2315−592 was discovered with *ASCA* during the observation of IRAS 23128−5919. The light curve shows a clear periodic modulation at 1.489 ± 0.013 hr. Follow-up phase-resolved optical spectroscopy confirmed coincidence of the rotational period of the white dwarf and the orbital period and identified AX J2315−592 as a new AM Her–type object.

The shape of the X-ray light curve is quasi-sinusoidal, the amplitude of which decreases with increasing X-ray energy, which is the property of intermediate polars. The X-ray emission at the maximum of the folded light curve has an optically thin thermal plasma emission spectrum with a temperature of 17 ± 4 keV with negligible absorption. The spectrum at the minimum, on the other hand, suffers from complex absorption. The X-ray light curve and the spectral characteristics indicate that a single accreting pole is always within the visible hemisphere of the white dwarf, and the rotational minimum occurs when the pole points toward the observer.

Subject headings: novae, cataclysmic variables — stars: white dwarfs — X-rays: stars

1. INTRODUCTION

Magnetic cataclysmic variables (MCVs) are binary systems consisting of a magnetized white dwarf ($B \sim 10^{5-7}$ G) and a companion star filling its Roche lobe. Matter spilled over the Roche lobe is captured by the magnetic field of the white dwarf and accretes preferentially onto the magnetic poles. Because the flow is highly supersonic, a standing shock wave is formed close to the white dwarf surface, where the gravitational energy is released and converted into heat. As a result, a hot plasma with temperature $\sim 10^8$ K is produced that radiates hard X-ray emission. The AM Her–type star or polar is a subclass of MCV in which the white dwarf has comparatively strong magnetic field strength ($B = 1–6 \times 10^7$ G; Cropper 1990). The strong magnetic field provides AM Her–type stars with several unique properties such as cyclotron emission in the infrared–optical wave band and the synchronous rotation of the white dwarf with the orbital motion.

In this Letter, we report the results of the *ASCA* observation of the new AM Her–type object AX J2315−592 discovered serendipitously during the observation of the infrared-luminous galaxy IRAS 23128−5919 and discuss a possible accretion-pole geometry.

2. OBSERVATIONS

ASCA has four identical X-ray telescopes (XRT; Serlemitsos et al. 1995), which have large effective areas up to 10 keV. A pair of Solid-state Imaging Spectrometers (SIS; Burke et al. 1991) and Gas Imaging Spectrometers (Ohashi et al. 1996; Makishima et al. 1996) are located on the focal plane. The SIS instruments were operated in 1-CCD mode throughout the observation, and the field of view is a square with a size of 11′ × 11′. The field of view of the GIS, on the other hand, is a circle with a radius of 25′.

AX J2315−592 was discovered by chance when *ASCA* was observing IRAS 23128−5919 during 1995 November 2 13:20–November 3 20:50 (UT). Follow-up optical observations (Thomas & Reinsch 1995) identified AX J2315−592 with one of the two 16–17 mag stars in the *ASCA* error circle of 1′ radius, the celestial position of which is $\alpha = 23^h15^m18^s.4$, $\delta = -59°10'27''$ (equinox J2000.0). The center of the field of view of the SIS instrument was offset from IRAS 23128−5919 by 2′.5. Unfortunately, AX J2315−592 is located approximately 10′ away from IRAS 23128−5919 and was out of the field of view of the SIS. Results in this Letter are thus obtained solely with the GIS. Hereafter, we refer to the two GIS systems as GIS2 and GIS3.

Data selection was made in the following way. X-ray photons from AX J2315−592 were accumulated within a circular region of 5′ radius centered on the source. The background was accumulated in an annular region that has the same angular distance from the XRT boresight as the source region. We have discarded the data taken while the spacecraft passes through high background regions such as the South Atlantic Anomaly and areas with cutoff rigidity less than 6 GeV counts^{-1}. Also, we do not use the data when the XRT points within 5° from the limb of Earth, in order to avoid absorption by Earth's atmosphere and the intrusion of scattered solar X-rays. With these screenings, some 34 ks of data remain.

In the following analysis, we use the GIS response matrices of version 4.0 and the XRT point-spread function and the effective area tables of version 2.0 as calibrational data of the instruments. In the spectral fitting, we use XSPEC 9.0 in the XANADU package.

3. PERIODICITY

The light curve in the band 0.7–10 keV obtained by adding data from the two GIS detectors is shown in Figure 1. A data gap occurs in every 96 minute satellite orbit because of the data screening. The light curve is characterized by a slow modulation with possibly recurrent intensity minima at ∼59,000, ∼64,000, ∼70,000, and ∼85,000 s. The averaged count rate is 0.66 counts s^{-1} for GIS2 plus GIS3 in the band 0.7–10 keV.

To search for periodicity of the dipping, we have performed folding analysis in the trial period range 3000–7000 s. We have also evaluated the arrival time of each dip and have obtained the period by correlating the dip number with the arrival time. With these two kinds of analysis, the X-ray period is found to

[1] Department of Astrophysics, Nagoya University, Chikusa-ku, Nagoya 464-01, Japan.
[2] Institute of Space and Astronautical Science, 3-1-1 Yoshinodai, Sagamihara, Kanagawa 229, Japan.

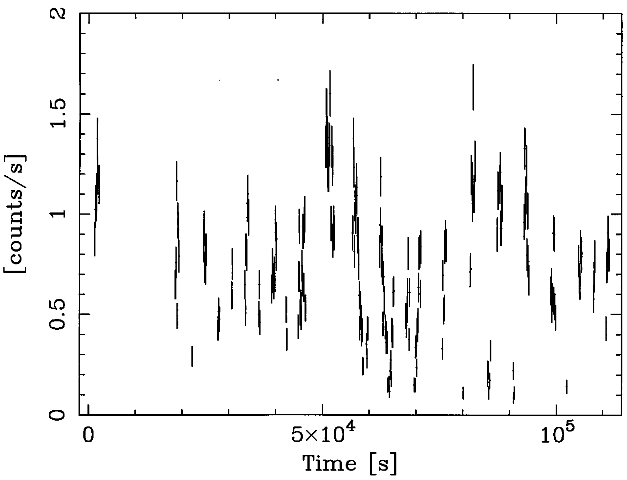

FIG. 1.—X-ray light curve of AX J2315−592 in the band 0.7–10 keV obtained with GIS2 + GIS3 with 128 s binning. The 1.49 hr modulation is clearly seen.

be 5359 ± 47 s, which is consistent with the period 5360 ± 10 s determined by the Doppler velocity curve of Hβ and He II narrow emission components (Thomas & Reinsch 1995), which are thought to originate from orbital-bound components such as the surface of the secondary or the gas stream in the orbital plane illuminated by the white dwarf. Thomas & Reinsch (1996) also found that broad components in the Hβ and He II emission lines, which are thought to originate from the preshock accretion column, vary at the same period as the narrow components and identify AX J2315−592 as a new AM Her–type star. The X-ray period that we found, representing the rotational period of the white dwarf, confirms this identification.

In Figure 2, we show the light curve folded at the optical period in three energy bands according to the ephemeris defined by Thomas & Reinsch (1996). The phase origin is defined as the blue to red crossing point of the narrow emission lines and thus corresponds to the inferior conjunction of the secondary star. The shape of the light curve is quasi-sinusoidal. The modulation amplitude is the greatest in the lowest energy band and gradually decreases with X-ray energy. If we fit the folded light curves by a sinusoid with the rotational period of the white dwarf, the half-amplitudes normalized by the average intensities are 87% ± 2%, 57% ± 2%, and 14% ± 4% in the bands 0.7–2.3 keV, 2.3–6.0 keV, and 6.0–10.0 keV, respectively (errors are at the 90% confidence level). Note that this property is rather like intermediate polars (Norton & Watson 1989). The modulation amplitude of an AM Her–type star is, on the other hand, almost constant with a slight decrease with decreasing X-ray energy (Ishida 1991). This is in the opposite sense to the observed modulation amplitude of AX J2315−592.

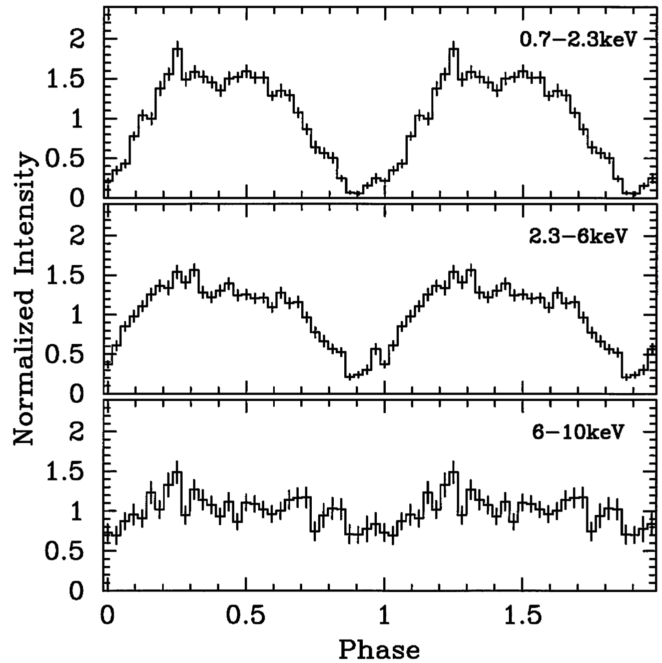

FIG. 2.—Light curves in the bands 0.7–2.3 keV, 2.3–6.0 keV, and 6.0–10.0 keV folded according to the ephemeris of Thomas & Reinsch (1996) in which the phase 0 corresponds to the inferior conjunction of the secondary star. The vertical axis is the intensity normalized by the average intensity. The modulation amplitude decreases with X-ray energy, which is 87% ± 2%, 57% ± 2%, and 14% ± 4%, respectively, from the fit with a sinusoid. Note that this property is rather like intermediate polars.

4. SPECTRAL ANALYSIS

We have made the X-ray spectra of ϕ = 0.23–0.63 (rotational maximum phase) and ϕ = 0.83–1.03 (rotational minimum phase) by adding the data from the two GIS detectors. They are shown in Figures 3*a* and 3*b*, respectively. First, we have fitted the rotational maximum phase spectrum with a power law and a Gaussian line, representing the iron emission line seen around 6–7 keV, and have found a photon index of 1.49 ± 0.06 (χ^2_ν = 0.94). The line central energy settles at $6.84^{+0.13}_{-0.09}$ keV, which indicates that the iron emission line is of thermal plasma origin. A huge line equivalent width of 900^{+300}_{-200} eV is obtained. Having established the thermal nature of the X-ray emission from the line central energy, we have adopted an optically thin thermal plasma emission model (Raymond & Smith 1977). The rotational maximum phase spectrum is well represented by this model with a temperature of 17 ± 4 keV (χ^2_ν = 0.96). The absorption is negligible, and only the upper limit of the hydrogen column density is determined ($N_H < 7 \times 10^{20}$ cm^{-2}).

The abundance determined by the iron Kα line is twice as great as solar and more than in EX Hya by a factor of 3 (Fujimoto & Ishida 1996). It should be noted, however, that the iron line emission from the plasma may be unisotropic because of resonance trapping (Done, Osborne, & Beardmore 1995). The amount of the unisotropy depends upon the density and the geometry of the accretion column and is unpredictable. The reflected emission from the white dwarf surface also possibly causes the overestimation of the abundance in two ways: the fluorescent iron Kα emission line at 6.4 keV (Beardmore et al. 1995; Ishida, Mukai, & Osborne 1994; Mukai, Ishida, & Osborne 1994; Hellier et al. 1996) and hardening of the continuum spectrum. However, we have confirmed that the former reduces the abundance by only ~10% by adding a narrow Gaussian line at 6.4 keV into the model (see the third row of Table 1). We consider that the latter effect is small either because the 6.4 keV line is relatively weak or because the observed continuum slope is steep.

The rotational minimum spectrum is, on the other hand, significantly harder than that of the rotational maximum spectrum; if we approximate it with a power law, the photon

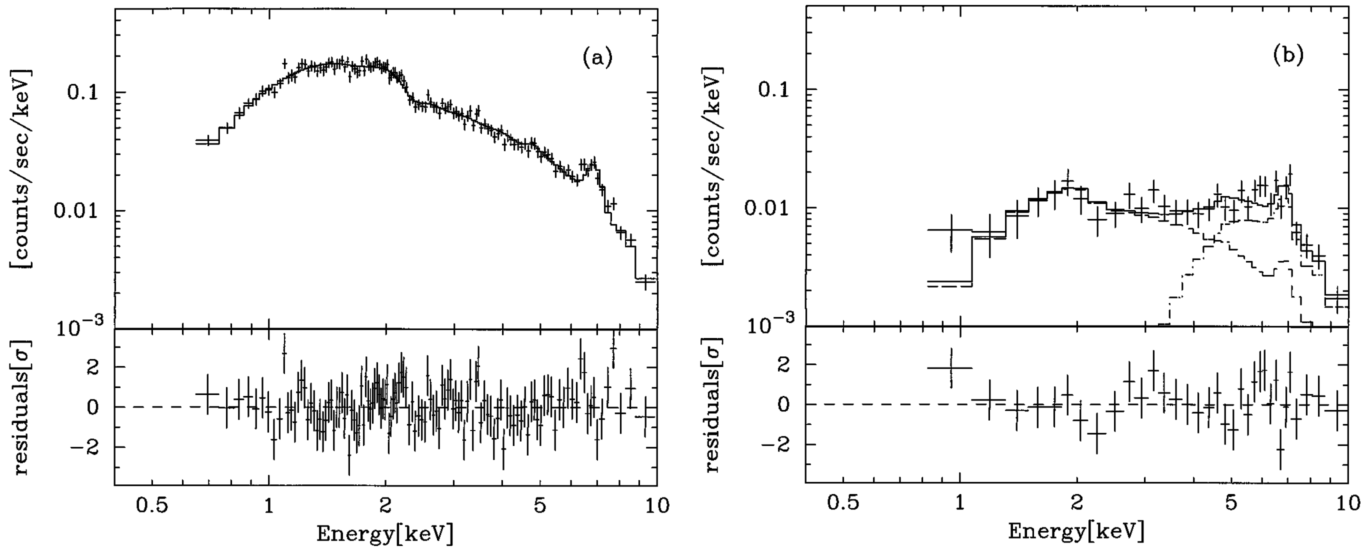

FIG. 3.—Spectrum of (*a*) the rotational maximum phase and (*b*) the rotational minimum phase together with the best-fit optically thin thermal plasma emission model (Raymond & Smith 1977) shown by histograms. Note that a partial-covering model is adopted in (*b*).

index becomes ~0. In Figure 4, we show the channel-to-channel ratio of the rotational minimum spectrum to that of the rotational maximum, together with curves of $e^{-N_{\rm H}(\sigma_a + \sigma_{\rm T})}$ for various hydrogen column densities, where σ_a and $\sigma_{\rm T}$ are the cross sections of photoelectric absorption and Thomson scattering, respectively. If the rotational minimum spectrum were expressed by the rotational maximum spectrum undergoing the absorption represented by a single column density, the channel-to-channel ratio of the rotational minimum spectrum to that of the rotational maximum would be aligned to one of the curves. We thus have introduced partial covering, as is conventionally done for MCVs, and have tried to fit the rotational minimum spectrum. The best-fit parameters are listed in Table 1. Because of statistical limitations, we have fixed the temperature and the abundance at the values obtained from the fit of the rotational maximum phase spectrum.

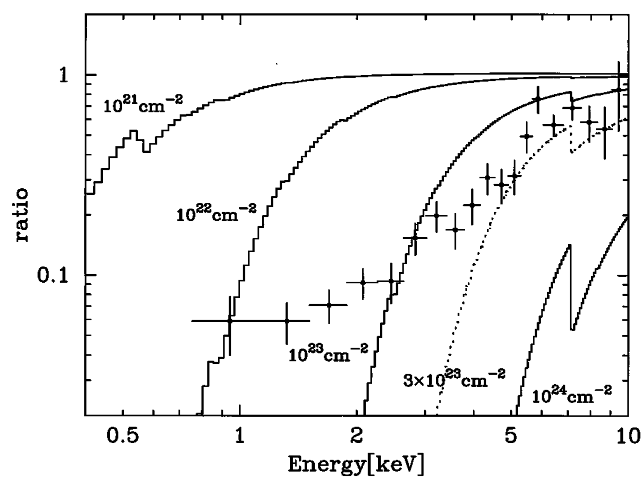

FIG. 4.—Channel-to-channel ratio of the rotational minimum (= dip) spectrum to that of the rotational maximum. X-ray transmissions expected for matter with hydrogen column densities of 10^{21}, 10^{22}, 10^{23}, 3×10^{23}, and 10^{24} cm^{-2} are superimposed. Electron scattering expected for an absorber with solar abundances is taken into account.

The partial covering absorber probably represents the inhomogeneous accretion geometry due to funneling of matter by the magnetic field and/or blobby accreting matter (Kuijpers & Pringle 1982; Frank, King, & Lasota 1988).

5. DISCUSSION

AX J2315−592 was detected for the first time by *ASCA* at the intensity level ~1.5 mCrab in the 2–10 keV bandpass. Although several X-ray observations have so far been made of the sky field around AX J2315−592, no X-ray source has previously been reported at this position; *HEAO-1* LASS gives an upper limit of 0.25 mCrab at 5 keV (Wood et al. 1984). A scanning observation by *Ginga* in 1989 June derived an upper limit of 0.2 mCrab in the band 2–10 keV (Awaki et al. 1996). Although an AM Her–type object is generally a strong EUV/soft X-ray source, AX J2315−592 is not listed in the *ROSAT* WFC catalog (Pounds, Shara, & McLean 1993), either. AX J2315−592 seems to have an unusually long low state.

As described in § 3, the energy dependence of the modulation amplitude of AX J2315−592 is atypical of AM Her–type stars and is rather like that of intermediate polars. The intermediate polar is the other subclass of MCV in which the white dwarf rotates asynchronously with the orbital revolution. Because of the asynchronism, two equivalent accreting poles are formed on the white dwarf surface, which are expected to be separated by 180° if the field configuration is dipole. In this situation, the X-ray flux of the intermediate polars cannot be modulated by the occultation of the poles because the deficit of the flux caused by the occultation of one pole is completely compensated by the appearance of the other pole. The intensity modulation is mainly caused by the absorption that occurs in the preshock accretion column when the accreting pole on the upper hemisphere becomes close to the line of sight, and the rotational maximum occurs when the upper pole points away from the observer. This idea is supported by the observations of *EXOSAT* (Norton & Watson 1989) and *Ginga* (Ishida 1991), in which the modulation amplitude decreases with X-ray energy, and is generally not more than 20% at about 10 keV.

This cannot, however, be true for AM Her–type stars

TABLE 1

BEST-FIT SPECTRAL PARAMETERS OF THE ROTATIONAL MAXIMUM PHASE AND THE ROTATIONAL MINIMUM PHASE SPECTRA WITH AN OPTICALLY THIN THERMAL PLASMA EMISSION MODEL (RAYMOND & SMITH 1977)

	OPTICALLY THIN THERMAL PLASMA EMISSION				IRON LINE			
PHASE (ϕ)	kT (keV)	Abundance[a]	N_H (10^{22} cm^{-2})	CF[b]	Central Energy (keV)	Width[c] (keV)	EW[d] (eV)	χ^2/dof
0.23–0.63 (max)......	$16.5^{+3.9}_{-3.1}$	$1.93^{+0.56}_{-0.43}$	<0.07	...	...	...	...	114/119
0.83–1.03 (min)......	16.5 (fixed)	1.93 (fixed)	32^{+15}_{-10}	$0.85^{+0.04}_{-0.05}$	...	...	...	32.8/30
			$1.1^{+0.7}_{-0.5}$	$0.15^{+0.05}_{-0.04}$				
0.23−0.63 (max).....	$17.2^{+4.5}_{-3.2}$	$1.76^{+0.61}_{-0.43}$	<0.06	...	6.40 (fixed)	0.0(fixed)	100^{+20}_{-60}	108/118

NOTE.—90% confidence errors are shown.
[a] Mostly determined from iron emission line.
[b] Covering fraction.
[c] Width of Gaussian line in σ.
[d] Equivalent width.

because of the synchronous rotation, which causes a considerable imbalance of mass accretion rate between the two magnetic poles. In fact, ST LMi (Beuermann, Stella, & Krautter 1984) and VV Pup (Osborne et al. 1984) are well-known AM Her–type stars in which accretion takes place onto a single magnetic pole. Even if the accretion takes place at two magnetic poles, the two accreting poles will never be separated by 180° because mass accretes along a closed magnetic field line. Because of these effects, the rotational X-ray intensity modulation in AM Her–type stars is mainly caused by the occultation of the main accretion pole. The modulation amplitude is almost energy independent and is more than 40% at about 10 keV in general.

In explaining the unusually small modulation amplitude of AX J2315−592 above 6 keV, we consider it is most likely that a single accretion pole on the upper hemisphere is always visible by the observer and never crosses behind the limb of the white dwarf. This idea is supported by the facts that the rotational minimum spectrum can be explained by the same intrinsic spectral model as the rotational maximum phase with extra partial covering and that the phase of the rotational minimum (= dip) and that of the inferior conjunction of the secondary coincide within $\Delta\phi < 0.1$. The latter strongly suggests that the accreting pole points toward the observer during the rotational minimum phase, which excludes the possibility that the rotational minimum (= dip) is caused by the occultation of the accreting pole by the white dwarf. Note that it is unique to AM Her–type objects that maximum flux occurs when the angle between the line of sight and the direction of the accretion flow is maximum, although it is standard for intermediate polars. We conclude it is likely that the only one accreting pole is seen in AX J2315−592, which never moves behind the limb of the white dwarf, and the intensity modulation is caused by absorption in the preshock accretion column. We expect this picture to be confirmed by optical polarimetry in the near future.

The authors would like to express their best gratitude to all the *ASCA* team members in conducting this observation. Y. T. thanks Japan Society for the Promotion of Science for support. This work was partly supported by the Grant-in-Aid for Scientific Research on Specially Promoted Research, contract No. 07102007, from the Ministry of Education, Science, Sports and Culture, Japan.

REFERENCES

Awaki, H., Yamauchi, S., Iwasawa, K., Kamata, Y., Koyama, K., & Tawara, Y. 1996, in preparation
Beardmore, A. P., Done, C., Osborne, J. P., & Ishida, M. 1995, MNRAS, 272, 749
Beuermann, K., Stella, L., & Krautter, J. 1984, in X-ray Astronomy '84, ed. M. Oda & R. Giacconi (Sagamihara: ISAS), 27
Burke, B. E., Mountain, R. W., Harrison, D. C., Bautz, M. W., Doty, J. P., Ricker, G. R., & Daniels, P. J. 1991, IEEE Trans., ED-38, 1069
Cropper, M. 1990, Space Sci. Rev., 54, 195
Done, C., Osborne, J. P., & Beardmore, A. P. 1995, MNRAS, 276, 483
Frank, J., King, A. R., & Lasota, J. P. 1988, A&A, 193, 113
Fujimoto, R., & Ishida, M. 1996, ApJ, submitted
Hellier, C., Mukai, K., Ishida, M., & Fujimoto, R. 1996, MNRAS, submitted
Ishida, M. 1991, Ph.D. thesis, Univ. of Tokyo
Ishida, M., Mukai, K., & Osborne, J. P. 1994, PASJ, 46, L81
Kuijpers, J., & Pringle, J. E. 1982, A&A, 114, L4
Makishima, K., et al. 1996, PASJ, 48, 171
Mukai, K., Ishida, M., & Osborne, J. P. 1994, PASJ, 46, 87
Norton, A. J., & Watson, M. G. 1989, MNRAS, 237, 853
Ohashi, T., et al. 1996, PASJ, 48, 157
Osborne, J., et al. 1984, in X-ray Astronomy '84, ed. M. Oda & R. Giacconi (Sagamihara: ISAS), 59
Pounds, K. A., Shara, D. J., & McLean, B. 1993, PASP, 105, 387
Raymond, J. C., & Smith, B. W. 1977, ApJS, 35, 419
Serlemitsos, P. J., et al. 1995, PASJ, 47, 105
Thomas, H.-C., & Reinsch, K. 1995, IAU Circ., 6261
———. 1996, in preparation
Wood, K. S., et al. 1984, ApJS, 56, 507